Research Paper

Algorithm-based analysis of collective decoherence in quantum search

Cyrus P. MASTER[1], Shoko UTSUNOMIYA[2], Yoshihisa YAMAMOTO[3]
[1,2,3]National Institute of Informatics, Tokyo, Japan
[1,3]E.L. Ginzton Laboratory, Stanford University, Stanford, CA
[2,3]Department of Information and Communication Engineering, The University of Tokyo, Tokyo, Japan

ABSTRACT

A major challenge in the implementation of quantum computers is mitigating the impact of undesired couplings with the environment that lead to decoherence. Here, we discuss an error-avoiding strategy that is based upon freedoms inherent in decomposing a quantum algorithm into fundamental gates. Although this approach is specific to a particular algorithm and a collective noise model, it does not the require complicated encodings or significant additional qubit resources of more general error-correcting codes. This paper also includes an overview of quantum computation, including a discussion of the quantum search algorithm.

KEYWORDS

Quantum computation, quantum error-correction, decoherence, quantum algorithms, spin-boson models, decoherenec-free subspaces

1 Introduction

In future quantum information processing systems, quantum bits (qubits) of information are likely to be stored in identical two-level systems (e.g. spins, or pseudospins) that are spatially separated to simultaneously allow independent control of single qubits and mutual interaction between qubits. In such systems, information is encoded in the delicate quantum correlations that exist between qubits, and is manipulated over time by unitary single and two-qubit operations. Unwanted interactions of the qubits with their environment can lead to errors in the computation result, either by energy-relaxation (i.e., dissipation or T_1 processes) or by degradation of relative phase information (i.e., decoherence or T_2 processes). To avoid such errors, an ideal quantum computer should be wholly shielded from its environment. However, as one needs to couple the qubits to the outside world to apply single and two-qubit operations, it is inevitable that a quantum computer will be prone to some residual environmental interactions that lead to decoherence.

A sophisticated theory of error-avoiding and error-correcting codes has been developed to protect the output of quantum computers from errors due to general dissipative and decohering processes. [1]–[20] Among these methods is the labeling of logical qubits in a decoherence-free subspace, in which the encoded information is immune to system-environment interactions. However, these methods require complicated encodings of information amongst the two-level systems and/or a large number of auxiliary qubits and intermediate measurements.

The error-avoiding technique discussed here leverages the fact that there is considerable freedom in the decomposition of a given quantum algorithm into a sequence of elementary single and two-qubit gates. As the quantum computer evolves in time, the collection of qubits traces out a path in its state space that depends upon the sequence of gates. In the absence of decoherence, all trajectories lead to the same final state. However, if there is undesired system-environment coupling, the final state is erroneous. Furthermore, the er-

Received January 31, 2006; Revised March 20, 2006; Accepted March 24, 2006.
1) *cpmaster@gmail.com*, 2) *shoko@nii.ac.jp*, 3) *yosihisa@stanford.edu*
DOI: 10.2201/NiiPi.2006.3.2

ror depends upon the chosen trajectory, and thus the elementary-gate sequence. If the system-environment interaction exhibits a high-degree of symmetry, a simple geometrical argument can be made to find a trajectory that minimizes the impact of decoherence for selected quantum algorithms. The strategy employed here leverages the idea of decoherence-free subspaces, in that the state is steered through a region of the Hilbert space in which the coupling between the system and environment is presumed to be minimal. However, unlike decoherence-free subspaces, this approach encodes qubits in the standard computational basis, avoiding the difficult encoding issues that complicate the implementation of the former.

The decoherence model considered here is collective in the sense that all qubits couple symmetrically with the environment. This model is applicable if the characteristic wavelength of the environment is longer than the largest physical distance between qubits. This model might be relevant for solid-state implementations, where qubits are two-level systems (e.g., selected ionic or atomic levels) that couple to long-wavelength modes of a cold phonon bath. The electric-dipole coupling of closely-spaced atoms to a fluctuating electromagnetic field is another such example.

As an example of this procedure, we demonstrate that a judicious decomposition of the quantum search algorithm can mitigate the impact of dissipation. While this is demonstrated for cases where the number of qubits is small, the geometric argument used to derive the gate decomposition extends to an arbitrary number of qubits.

It should be emphasized that this strategy does not constitute a general, scalable method of error-correction. However, it does highlight the fact that the intrinsic physical interactions coupling qubits to their environment should play a role in determining how sequences of gates should be composed. Furthermore, we might envision a testbed quantum computer, composed of a few tens of qubits, for which the overhead required to implement error-correcting codes is steep. In other words, if we redundantly encode each qubit using five physical two-level systems, we may not have many logical qubits to work with. In such a case, an alternative means to mitigate decoherence is advisable, such as the scheme described in this paper.

To aid readers outside of the field of quantum computation, Sec. 2 provides an extended background of relevant topics. In particular, we address the following fundamental questions:

- What distinguishes quantum computation from "classical" computers?
- What are the required elements of a quantum computer?
- Why might quantum computers be useful, and for what applications? In other words, which algorithms are interesting?

In Sec. 3, we introduce a parameter to qualitatively describe the instantaneous dissipation rate due a collective interaction with a reservoir of boson modes. A modification to the quantum search algorithm is proposed based upon its geometric structure, and the average dissipation rates of the original and modified algorithms are compared.

2 Background

2.1 Classical and quantum computers

Before venturing into a description of quantum computers, it is convenient to first discuss a classical model for computing machines. While the Turing machine [21], [22] is of great historical and theoretical importance, a model based on *Boolean circuits* is a more accurate representation of everyday desktop and laptop computers. In the latter model, a computer consists of a collection of n binary variables, or bits. An algorithm is represented by a network of Boolean gates that performs a sequence of logic operations on the binary inputs. Of seminal importance is the fact that arbitrary computable functions can be constructed out of a finite set of primitive circuit elements, or gates. One common set [23] consists of a FANOUT gate that copies one bit to two, a gate to exchange two input bits, and the NAND gate, which is the composition of the Boolean AND and NOT gates.

The complexity of a given algorithm is quantified by the number of primitive gates required to generate an output[1)]. If the number of gates scales polynomially with the number of bits n, the algorithm is deemed *efficient*. While this criterion may seem arbitrary, it has two important advantages. First, the composition of two efficient algorithms is itself efficient, as polynomials are closed under composition. Thus, a complicated efficient algorithm can be constructed from efficient subroutines. Second, the *modern* or *strong Church-Turing thesis* conjectures that the time required for one computational model to evaluate a computable function is a polynomial function of the time required by any other computational model. If true, the strong Church-Turing thesis implies that the notion of efficiency is universal. If an efficient algorithm can be found for a given problem, the strong Church-Turing thesis would imply that the problem may be solved efficiently by all physically reasonable computational models.

A quantum computer can be defined by a generaliza-

[1)] This metric is equivalent to the total computation time, assuming that each primitive gate requires a constant time to execute.

tion of the Boolean circuit model for computation [23], [24]. Consider a collection of n two-level quantum systems (qubits); each two-dimensional complex vector space is spanned by the kets $|0\rangle$ and $|1\rangle$. The overall 2^n dimension Hilbert space is spanned by the *computational basis vectors* $|\underline{x}\rangle$, where $\underline{x} \in \{0, 1, 2, \cdots, 2^n - 1\}$. The underline denotes that the state of each qubit may be inferred from the n-bit binary string for the integer x.

It is assumed that each qubit is initialized in the fiducial $|0\rangle$ state at the outset of a computation. Logic operations consist of a sequence of unitary transformations (i.e. gates) on single qubits or pairs of qubits[2]. A primitive set of gates can be chosen to allow arbitrary unitary transformations; such sets are *universal*. One universal set consists of all single-qubit gates along with the *controlled-NOT* gate, which maps the two-qubit state $|x, y\rangle$ to $|x, x \oplus y\rangle$, where $\oplus$ denotes the exclusive-OR operation. The output of the computation is derived by the projective measurement of the qubits in the computational basis. This model is often denoted as the *standard model of quantum computation*.

The standard model subsumes the classical Boolean circuit model. This statement seems problematic at first, as unitary operations are invertible, whereas Boolean gates such as NAND are irreversible. However, a classical circuit can use reversible gates with no loss of power by adding a reasonable number of scratch bits. [25], [26] Thus, any efficient algorithm on a classical computer can be translated into an efficient algorithm on a quantum computer given sufficient ancillary qubits. It is the lack of a converse statement that makes quantum computation so interesting. Indeed, there exist problems for which an efficient quantum algorithm is known with no classical counterpart, calling the strong Church-Turing thesis into question (for reviews of elementary quantum algorithms, refer to Refs. [23], [27], [28]). Integer factorization [29], [30] is one such example. Furthermore, the computation time of search problems can be dramatically reduced by quantum algorithms, as is discussed in the next subsection.

2.2 Quantum search algorithms

Grover's unstructured database search algorithm [31], [32] is one of several algorithms discovered in the mid-nineties that spurred great interest in the potential computational power of quantum computers relative to their classical counterparts. Although the utility of the algorithm lies in its application as a building block in other problems, it is easiest for us to analyze with the algorithm in its original form, with a slight modification [33] to allow for multiple target states.

We are given a function $f : \mathbb{Z}_N \to \{0, 1\}$ that maps the integers 0 through $N - 1$, where $N = 2^n$, to a single Boolean output. We are told there exists a nonempty set for which the function yields output 1:

$$X = \{x | f(x) = 1\},\ |X| \equiv r,\ 0 < r < N. \tag{1}$$

Given a black box that can be queried for function evaluations of $f(x)$, we seek an element of X with a minimum expected number of queries over all f. The function $f(x)$ can be thought of as a database with unknown structure for which the subset X of inputs are desired records, or *targets*. An obvious heuristic is to guess values of x at random; $O(N/r)$ evaluations will find a solution with a minimum guaranteed probability of success.

A quantum algorithm in the standard model can solve an equivalent problem with $O(\sqrt{N})$ invocations of an oracle $\hat{U}_X$, which encodes the function $f(x)$ as a unitary operator. $\hat{U}_X$ is defined on an n-qubit Hilbert space:

$$\hat{U}_X = \sum_{x=0}^{N-1} (-1)^{f(x)} |\underline{x}\rangle \langle \underline{x}| = \hat{I} - 2 \sum_{x \in X} |\underline{x}\rangle \langle \underline{x}|, \tag{2}$$

where $\hat{I}$ is the identity operator, and the second summation includes computational basis states $\left\{|\underline{0}\rangle, |\underline{1}\rangle, \cdots, |\underline{N-1}\rangle\right\}$ that are targets. Acting on a general n-qubit state, $\hat{U}_X$ shifts the phase of target components by π, and does nothing to remaining components.

Consider the operator $\hat{Q} = -\hat{H}\hat{U}_0\hat{H}\hat{U}_X$ acting on an N-dimensional Hilbert space; $\hat{H}$ is the Hadamard operator on all n qubits, and $\hat{U}_0$ flips the phase of the $|\underline{0}\rangle$ state:

$$\hat{U}_0 = \hat{I} - 2 |\underline{0}\rangle \langle \underline{0}|. \tag{3}$$

Note that $\hat{H}$ is self-inverse, so $\hat{H} = \hat{H}^\dagger$. Define the equal superposition state $|\sigma\rangle$ and the superposition state over all targets $|\bar{X}\rangle$:

$$|\sigma\rangle = \hat{H} |\underline{0}\rangle = \frac{1}{\sqrt{N}} \sum_{x=0}^{N-1} |\underline{x}\rangle \tag{4a}$$

$$|\bar{X}\rangle = \frac{1}{\sqrt{r}} \sum_{x \in X} |\underline{x}\rangle \tag{4b}$$

$\hat{Q}$ leaves invariant the two-dimensional subspace Q_0 spanned by $|\sigma\rangle$ and $|\bar{X}\rangle$; i.e., $\hat{Q} = Q_0 \oplus Q_0^\perp$. This is easily verified, as

$$\hat{Q}|\sigma\rangle = -\hat{H}\left(\hat{I} - 2|\underline{0}\rangle\langle\underline{0}|\right)\hat{H}\left(1 - 2\sum_{x \in X} |\underline{x}\rangle\langle\underline{x}|\right)|\sigma\rangle$$

[2] As each two-level qubit can be considered as a spin or pseudospin, transformations can be expressed using the Pauli operators $\hat{\sigma}^x$, $\hat{\sigma}^y$ and $\hat{\sigma}^z$.

$$= -(1 - 2|\sigma\rangle\langle\sigma|)\left(1 - 2\sum_{x\in X}\left|\underline{x}\right\rangle\left\langle\underline{x}\right|\right)|\sigma\rangle \tag{5a}$$

$$= \left(1 - \frac{4r}{N}\right)|\sigma\rangle + 2\sqrt{\frac{r}{N}}\left|\bar{X}\right\rangle, \tag{5b}$$

$$\tag{5c}$$

and

$$\hat{Q}\left|\bar{X}\right\rangle = \left|\bar{X}\right\rangle - 2\sqrt{\frac{r}{N}}|\sigma\rangle\,. \tag{6}$$

Let $\left|\bar{X}^{\perp}\right\rangle$ be a vector in the invariant subspace such that $\left|\bar{X}^{\perp}\right\rangle$ is orthogonal to $\left|\bar{X}\right\rangle$:

$$\left|\bar{X}^{\perp}\right\rangle = \sqrt{\frac{N}{N-r}}|\sigma\rangle - \sqrt{\frac{r}{N-r}}\left|\bar{X}\right\rangle. \tag{7}$$

The matrix representation of $\hat{Q}$ on the two-dimensional subspace spanned by $\left|\bar{X}\right\rangle$ and $\left|\bar{X}^{\perp}\right\rangle$ is then

$$\hat{Q} = \begin{bmatrix} 1 - \dfrac{2r}{N} & -\dfrac{2\sqrt{r(N-r)}}{N} \\ \dfrac{2\sqrt{r(N-r)}}{N} & 1 - \dfrac{2r}{N} \end{bmatrix}. \tag{8}$$

As the determinant of the matrix is 1, each invocation of Q_0 is a rotation by an angle θ, where

$$\theta = \sin^{-1}\left(\frac{2\sqrt{r(N-r)}}{N}\right), \tag{9}$$

which approaches $2/\sqrt{N}$ for $N \gg r$. Note that the angle between $|\sigma\rangle$ and $\left|\bar{X}\right\rangle$ is

$$\cos^{-1}\left|\langle\sigma|\,\bar{X}\right\rangle\right| = \cos^{-1}\left(\frac{1}{\sqrt{N}}\right), \tag{10}$$

which approaches $\pi/2$ if $N \gg r$. Thus, the number of iterations K of $\hat{Q}$ required to rotate $|\sigma\rangle$ to the state $\left|\bar{X}\right\rangle$ is

$$K = \frac{\cos^{-1}\left(1/\sqrt{N}\right)}{\theta} \approx \frac{\pi\sqrt{N}}{4}. \tag{11}$$

To find a target state with near unity probability, the system is initialized in the $|\sigma\rangle = H\left|\underline{0}\right\rangle$ state, K iterations of $\hat{Q}$ are performed, requiring $O(\sqrt{N})$ oracle calls, and projective measurement in the computational basis is carried out. The measurement of the n qubits yields the n-bit representation of a target state in set X with near certainty.

Brassard and Høyer [34] and Grover [35] showed that the search algorithm can be generalized, in that there is freedom to modify the initial state and Hadamard operations. To be precise, consider the operator

$$\hat{Q}' = -\hat{V}\hat{U}_{\gamma}\hat{V}^{\dagger}\hat{U}_{X}, \tag{12}$$

where $\hat{V}$ is any unitary operator on all n qubits, $\hat{U}_{\gamma}$ is defined by

$$\hat{U}_{\gamma} = \hat{I} - 2|\gamma\rangle\langle\gamma|\,, \tag{13}$$

and $|\gamma\rangle$ is the initial state. A little algebra shows that the two-dimensional subspace spanned by $\hat{V}|\gamma\rangle$ and $\sum_{x\in X} V_{x\gamma}\left|\underline{x}\right\rangle$ are invariant under $\hat{Q}'$, where

$$V_{x\gamma} = \left\langle\underline{x}\right|\hat{V}|\gamma\rangle\,. \tag{14}$$

$\hat{V}$ causes a rotation in the invariant subspace by an angle

$$\sin^{-1}\left[2\sqrt{\sum_{x\in X}\left|V_{x\gamma}\right|^2 - \left(\sum_{x\in X}\left|V_{x\gamma}\right|^2\right)^2}\right] \tag{15}$$

The generalized algorithm can be useful in a couple ways. First, if the problem that we wish to solve is a search problem with a known structure, it may hold that $\hat{V}$ can be chosen to reduce the number of required calls to the oracle. For example, Grover [36] showed that if it is known that the target states are a fixed Hamming distance k from a known n-bit string $\underline{y}$, then the number of required iterations can be reduced by selecting $|\gamma\rangle = \left|\underline{y}\right\rangle$ and defining the single-qubit operator $\hat{V}$ as

$$\hat{V} = \begin{bmatrix} \sqrt{1-k/n} & \sqrt{k/n} \\ \sqrt{k/n} & -\sqrt{1-k/n} \end{bmatrix}. \tag{16}$$

Second, as we will discuss in Sec. 3, replacement of Hadamard gates in the unstructured search algorithm with other single qubit gates that preserve $V_{xy} = 1/\sqrt{N}$ can be advantageous in reducing the impact of decoherence. Such modifications do not modify the gate count of the unstructured search algorithm, but could be beneficial if unwanted interactions are present between the system and the environment.

3 Error avoidance by gate design

In the standard model of quantum computation, an algorithm such as quantum search is implemented by decomposing the unitary evolution into a sequence of single-qubit and two-qubit unitary gates. This decomposition is not unique; there is an infinite variety of ways to expand a given unitary operation as a sequence of single-qubit and controlled-NOT gates. Ideally, one would employ a general optimization procedure in which the gate decomposition for a particular algorithm is manipulated until the error due to unwanted system-environment interaction is minimized.

However, such an approach is not feasible, as each gate decomposition must be explicitly simulated on a classical computer to compute the error. Simulation of a quantum circuit on a classical computer is generally inefficient due to the exponential size of the Hilbert space. The approach of mitigating decoherence by gate design is useful only if both the algorithm and the decoherence model possess a structure that immediately suggests an advantageous gate decomposition. In this section, we examine the quantum-search algorithm as such as example, in the presence of a collective, dissipative system-environment interaction.

3.1 Dissipation model

A general hamiltonian for the system and environment is

$$\hat{H} = \hat{H}_S \otimes \hat{I}_E + \hat{I}_S \otimes \hat{H}_E + \hat{H}_{SE}. \tag{17}$$

We consider the environment to be composed of a reservoir of boson modes, such that

$$\hat{H}_E = \sum_k \omega_k \left(\hat{a}_k^\dagger \hat{a}_k + 1/2\right). \tag{18}$$

For the system-reservoir interaction, we assume a simple model to reflect the exchange of energy between the qubits and the environment. The n qubits are coupled to the environment by a Jaynes-Cummings-like interaction

$$\hat{H}_{SE} = \frac{1}{2}\sum_{i=1}^{n}\sum_k \left(g_{i,k}^* \hat{\sigma}_i^+ \otimes \hat{a}_k + g_{i,k}\hat{\sigma}_i^- \otimes \hat{a}_k^\dagger\right). \tag{19}$$

which may reflect the physical scenario of two-level atoms dipole-coupled to an external bosonic field. This interaction leads to energy exchange between the qubits and the reservoir, as the raising and lowering operators $\hat{\sigma}^+$ and $\hat{\sigma}^-$ lead to bit-flips.

We assume that the n qubits interact collectively with the reservoir, such that $g_{i,k} = g_k$. Defining the total spin operator $\hat{S}^\alpha = \frac{1}{2}\sum_{i=1}^{n} \hat{\sigma}_i^\alpha$, this implies that

$$\hat{H}_{SE} = \sum_k \left(g_k^* \hat{S}^+ \otimes \hat{a}_k + g_k \hat{S}^- \otimes \hat{a}_k^\dagger\right). \tag{20}$$

Furthermore, we assume that the reservoir is at zero temperature, so that each environment mode is in the vacuum state, which we denote as $|0\rangle_E$. We notate as $|k\rangle_E$ the reservoir state where all modes are in the ground state except for mode k, which has one excitation (e.g., a single phonon in mode k for vibrational modes in a solid-state system). Consideration of the single-excitation manifold will be sufficient to derive a first-order transition rate.

This collective interaction corresponds to the physical scenario in which the qubits are closely spaced relative to the wavelength of the cold reservoir.

In the interaction picture associated with $\hat{I}_S \otimes \hat{H}_E$, the hamiltonian is

$$\hat{H}^{\text{int}} = \hat{H}_S \otimes \hat{I}_E + \left(g_k^* e^{-i\omega_k t}\hat{S}^+ \otimes \hat{a}_k + g_k e^{i\omega_k t}\hat{S}^- \otimes \hat{a}_k^\dagger\right). \tag{21}$$

As the system-environment hamiltonian is expressed entirely in terms of the total spin operators, it is convenient to use the so-called collective angular momentum state (or Dicke-state) basis, as opposed to the computational basis.

3.2 Collective angular momentum states

Consider a collection of n spin-1/2 particles. One complete set of basis states consists of the tensor product of $\hat{\sigma}_i^z$ eigenstates for all spins i; these are the individual "spin-up" states $|\uparrow\rangle$ or "spin-down" states $|\downarrow\rangle$ for each two-level system. Alternatively, we can consider the simultaneous eigenstates of the total squared angular momentum operator and the total z-component angular operator. To be precise, define

$$\hat{J}^\gamma = \frac{1}{2}\sum_{i=1}^{n} \hat{\sigma}_i^\gamma \tag{22}$$

for $\gamma \in \{x, y, z\}$,

$$\hat{J}^2 = \left(\hat{J}^x\right)^2 + \left(\hat{J}^y\right)^2 + \left(\hat{J}^z\right)^2, \tag{23}$$

and $\hat{J}^\pm = \hat{J}^x + i\hat{J}^y$. The Cartesian operators satisfy the commutation relations

$$\left[\hat{J}^\alpha, \hat{J}^\beta\right] = i\epsilon^{\alpha\beta\gamma}\hat{J}^\gamma, \tag{24}$$

where $\epsilon_{\alpha\beta\gamma}$ is the antisymmetric Levi-Cevita tensor. Recognizing Eq. 24 as the fundamental commutation relations for angular momentum, we immediately know that there exist simultaneous eigenstates $|j, m, \alpha\rangle$ of $\hat{J}^2$ and $\hat{J}^z$ such that

$$\begin{aligned}\hat{J}^2|j, m, \alpha\rangle &= j(j+1)|j, m, \alpha\rangle \\ \hat{J}^z|j, m, \alpha\rangle &= m|j, m, \alpha\rangle\end{aligned} \tag{25}$$

for half-integral j and $m \in \{-j, -j+1, \cdots, j\}$. The label α distinguishes degenerate states, and will be labeled by positive integers.

The allowed states and their degeneracies can be computed by the theory of addition of angular momentum. For the case of n spin-1/2 particles, the calculation is particularly simple. First, note that the tensor product of n spin-up/spin-down states is an eigenstate of $\hat{J}^2$ with eigenvalue m in the set $\{-n/2, -n/2+1, \cdots, n/2\}$. Thus, $j \in \{n/2, n/2-1, \cdots, 0\ (1/2)\}$; the minimum value of

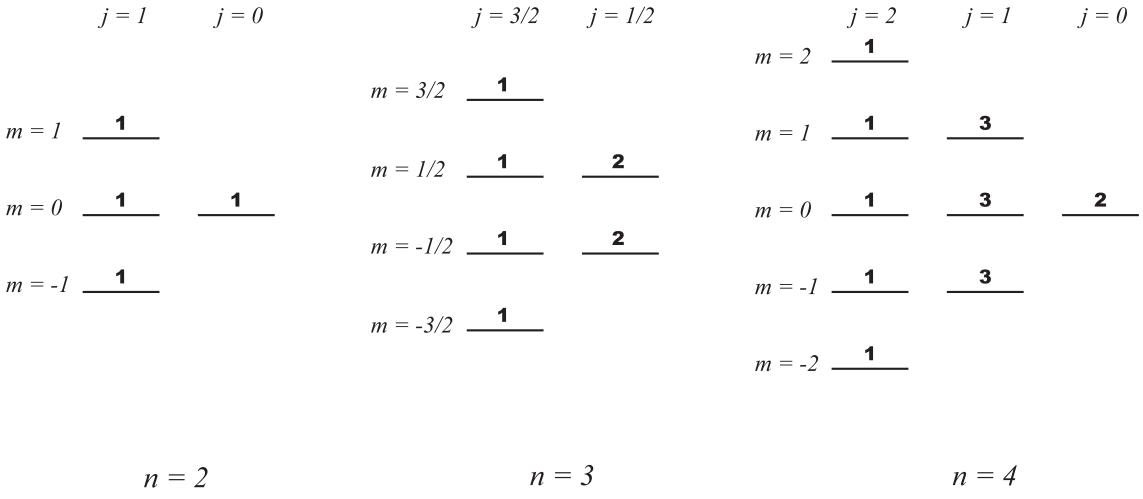

Fig. 1 Collective angular momentum states for $n = 2, 3, 4$. The degeneracy of each state is indicated in bold.

j depends on whether n is even or odd. The allowed values of j and m can be represented graphically, as in Fig. 1

Before examining simple examples, first note that the fundamental commutation relations imply that $\left[\hat{J}^z, \hat{J}^+\right] = \hat{J}^+$. Thus,

$$\hat{J}^z\left(\hat{J}^+ |j,m,\alpha\rangle\right) = \left(\hat{J}^+\hat{J}^z + \hat{J}^+\right)|j,m,\alpha\rangle = (m+1)\hat{J}^+ |j,m,\alpha\rangle\,, \tag{26}$$

implying that $\hat{J}^+ |j,m,\alpha\rangle$ is also an eigenstate of $\hat{J}^2$ and $\hat{J}^z$, unless $\hat{J}^+ |j,m,\alpha\rangle = 0$. The eigenvalue j is unmodified, and $m \to m+1$. Similarly,

$$\hat{J}^- |j,m,\alpha\rangle = c\,|j,m-1,\alpha\rangle \tag{27}$$

where c is an as-yet undetermined constant. As $|j,m-1,\alpha\rangle$ is normalized,

$$|c| = \sqrt{\langle j,m,\alpha|\,\hat{J}^+\hat{J}^-\,|j,m,\alpha\rangle}. \tag{28}$$

From Eq. 23 and the commutation relations in Eq. 24, it can be shown that

$$\hat{J}^+\hat{J}^- = \hat{J}^2 - \left(\hat{J}^z\right)^2 + \hat{J}^z. \tag{29}$$

Thus,

$$|c| = \sqrt{j(j+1) - m^2 + m} = \sqrt{j(j+1) - m(m-1)}. \tag{30}$$

A similar derivation for $\hat{J}^+$ yields

$$\hat{J}^- |j,m,\alpha\rangle = \sqrt{j(j+1) - m(m-1)}\,|j,m-1,\alpha\rangle \tag{31a}$$

$$\hat{J}^+ |j,m,\alpha\rangle = \sqrt{j(j+1) - m(m+1)}\,|j,m+1,\alpha\rangle\,, \tag{31b}$$

Consider the simplest example, where $n = 2$. Amongst all four possible tensor products of spin-up/spin-down states, there only exists one for which $m = -1$, so

$$|j=1; m=-1; \alpha=1\rangle = |\downarrow\downarrow\rangle\,. \tag{32}$$

Successively applying $\hat{J}^+ = \frac{1}{2}(\hat{\sigma}_1^+ + \hat{\sigma}_2^+)$, we find

$$\begin{aligned} |j=1; m=0; \alpha=1\rangle &= \frac{|\downarrow\uparrow\rangle + |\uparrow\downarrow\rangle}{\sqrt{2}} \\ |j=1; m=1; \alpha=1\rangle &= |\uparrow\uparrow\rangle\,. \end{aligned} \tag{33}$$

The $|j=0; m=0\rangle$ states consist of all independent spin states with as many spins up as down that are orthogonal to $|j=1; m=0; \alpha=1\rangle$. There is only one such state, which is the singlet

$$|j=0; m=0; \alpha=1\rangle = \frac{|\downarrow\uparrow\rangle - |\uparrow\downarrow\rangle}{\sqrt{2}}. \tag{34}$$

For $n = 3$, we again deduce that the only state for which $m = -3/2$ has all spins down. The $j = 3/2$ manifold is then computed by successive applications of $\hat{J}^+$,

$$\begin{aligned} |j=3/2; m=-3/2; \alpha=1\rangle &= |\downarrow\downarrow\downarrow\rangle \\ |j=3/2; m=-1/2; \alpha=1\rangle &= \frac{|\downarrow\downarrow\uparrow\rangle + |\downarrow\uparrow\downarrow\rangle + |\uparrow\downarrow\downarrow\rangle}{\sqrt{3}} \\ |j=3/2; m=1/2; \alpha=1\rangle &= \frac{|\downarrow\uparrow\uparrow\rangle + |\uparrow\downarrow\uparrow\rangle + |\uparrow\uparrow\downarrow\rangle}{\sqrt{3}} \end{aligned}$$

$$|j=3/2;m=3/2;\alpha=1\rangle = |\uparrow\uparrow\uparrow\rangle\,. \tag{35}$$

There are three configurations where a single spin points down, and thus three degenerate states for $m = -1/2$. The $j = 1/2$, $m = -1/2$ subspace is two-fold degenerate, and spanned by kets orthogonal to the $j = 3/2$, $m = -1/2$ subspace. Thus,

$$\begin{aligned}
|j=1/2;m=-1/2;\alpha=1\rangle &= \frac{2\,|\downarrow\downarrow\uparrow\rangle + |\downarrow\uparrow\downarrow\rangle - |\uparrow\downarrow\downarrow\rangle}{\sqrt{6}} \\
|j=1/2;m=-1/2;\alpha=2\rangle &= \frac{|\downarrow\uparrow\downarrow\rangle - |\uparrow\downarrow\downarrow\rangle}{\sqrt{2}}
\end{aligned} \tag{36}$$

$$\begin{aligned}
|j=1/2;m=1/2;\alpha=1\rangle &= \frac{-2\,|\uparrow\uparrow\downarrow\rangle + |\uparrow\downarrow\uparrow\rangle + |\downarrow\uparrow\uparrow\rangle}{\sqrt{6}} \\
|j=1/2;m=1/2;\alpha=2\rangle &= \frac{-|\uparrow\downarrow\uparrow\rangle + |\downarrow\uparrow\uparrow\rangle}{\sqrt{2}}.
\end{aligned} \tag{37}$$

This procedure can be continued in a similar fashion for larger n. For $n = 4$, we list only the two-fold degenerate $j = 0$, $m = 0$ singlet states:

$$\begin{aligned}
&|j=0;m=0;\alpha=1\rangle \\
&\quad = \frac{|\uparrow\downarrow\uparrow\downarrow\rangle - |\uparrow\downarrow\downarrow\uparrow\rangle - |\downarrow\uparrow\uparrow\downarrow\rangle + |\downarrow\uparrow\downarrow\uparrow\rangle}{2} \\
&|j=0;m=0;\alpha=2\rangle \\
&\quad = \frac{2\,|\uparrow\uparrow\downarrow\downarrow\rangle + 2\,|\downarrow\downarrow\uparrow\uparrow\rangle - |\uparrow\downarrow\uparrow\downarrow\rangle - |\downarrow\uparrow\downarrow\uparrow\rangle - |\uparrow\downarrow\downarrow\uparrow\rangle - |\downarrow\uparrow\uparrow\downarrow\rangle}{\sqrt{12}}
\end{aligned} \tag{38}$$

3.3 Collective dissipation enhancement factor

The hamiltonian $\hat{H}^{\text{int}}$ leads to transitions between the collective angular momentum states $|j,m,\alpha\rangle_S$. These transitions can be explained by a simple first-order perturbation theory argument. [37], [38] Assume that at time $t = 0$, the system and environment are in the state $|j,m,\alpha\rangle_S \otimes |0\rangle_E$, which we compactly notate as $|j,m,\alpha;0\rangle$. A general state (limited to the single-excitation manifold) is

$$|\psi\rangle_{SE} = \sum_{j,m,\alpha}\left(c_{j,m,\alpha;0}\,|j,m,\alpha;0\rangle + \sum_k c_{j,m,\alpha;k}\,|j,m,\alpha;k\rangle\right). \tag{39}$$

The coefficients evolve under the Schrödinger equation

$$\begin{aligned}
&i\dot{c}_{j',m',\alpha';k'}(t) \\
&\quad = \sum_{j'',m'',\alpha'',k''} c_{j'',m'',\alpha'';k''}(t)\,\langle j',m',\alpha';k'|\hat{H}^{\text{int}}\,|j'',m'',\alpha'';k''\rangle\,.
\end{aligned} \tag{40}$$

Near $t = 0$,

$$c_{j'',m'',\alpha'',k''}(t) = \delta_{j,j''}\delta_{m,m''}\delta_{\alpha,\alpha''}\delta_{k,0}, \tag{41}$$

implying

$$\dot{c}_{j',m',\alpha';k'}(t) = -i\,\langle j',m',\alpha';k'|\,\hat{H}^{\text{int}}\,|j,m,\alpha;0\rangle\,. \tag{42}$$

Now, assume that no control hamiltonian is applied, so $\hat{H}_S$ is zero. Then, from Eq. 21,

$$\begin{aligned}
&\dot{c}_{j',m',\alpha';k'}(t) \\
&\quad = -i\sum_k g_k e^{i\omega_k t}\,\langle j',m',\alpha';k'|\,\hat{S}^-\otimes\hat{a}_k^\dagger\,|j,m,\alpha;0\rangle \\
&\quad = -i\sum_k g_k e^{i\omega_k t}\,\langle j',m',\alpha'|\,\hat{S}^-\,|j,m,\alpha\rangle\langle k'|\,\hat{a}_k^\dagger\,|0\rangle
\end{aligned} \tag{43}$$

where we have noted that $\hat{a}_k$ acting on the vacuum state is zero. The first matrix element is obtained from Eq. 31a,

$$\begin{aligned}
&\langle j',m',\alpha'|\,\hat{S}^-\,|j,m,\alpha\rangle \\
&\quad = \sqrt{j(j+1)-m(m-1)}\,\delta_{j,j'}\delta_{m-1,m'}\delta_{\alpha,\alpha'},
\end{aligned} \tag{44}$$

while the second matrix element is simply $\delta_{k,k'}$. Substituting Eq. 44 into Eq. 43 and integrating from 0 to t,

$$\left|c_{j,m-1,\alpha,k'}\right|^2 = \frac{[j(j+1)-m(m-1)]\,|g_{k'}|^2\sin^2(\omega_{k'}t)}{\omega_{k'}^2}. \tag{45}$$

By probability conservation, the population of the original qubit state $|j,m,\alpha\rangle$ decays as

$$\left|c_{j,m,\alpha,0}\right|^2 = 1 - E(j,m)\sum_{k'}\frac{|g_{k'}|^2\sin^2(\omega_{k'}t)}{\omega_{k'}^2}, \tag{46}$$

where

$$E(j,m) \equiv j(j+1) - m(m-1). \tag{47}$$

$E(j,m)$ is a collective enhancement factor that can augment or reduce the transition rate; it is the source of "superradiance" in quantum optics. [39] Note that for a single qubit (i.e., pseudospin) in the excited state $|j = 1/2, m = 1/2\rangle$, the collective enhancement factor is 1. Thus, $E(j,m)$ represents the enhancement in the transition rate compared to a single spin.

The collective enhancement factors are depicted in Fig. 2 for $n = 8$. The states $|j;m=-j;\alpha\rangle$ have $E(j,m) = 0$; no transitions can occur in these "subradiant" or "dark" states as $\hat{S}^-\,|j;m=-j;\alpha\rangle = 0$. Indeed, these states form the decoherence-free subspace for the hamiltonian in Eq. 19. By contrast, the states $|j = n/2; m = 0 \text{ or } \pm 1/2;\alpha\rangle$ are superradiant and have significantly higher dissipation rates than independent spins.

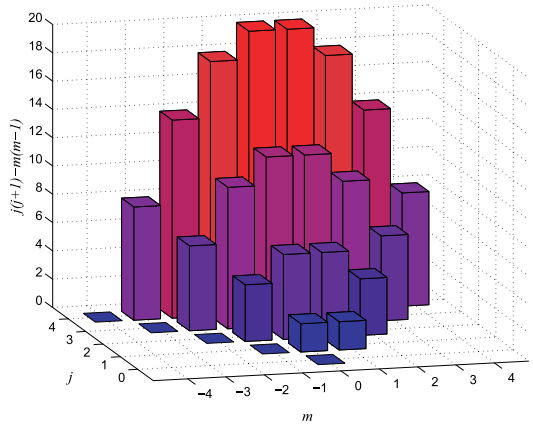

Fig. 2 The collective enhancement factor $j(j+1) - m(m-1)$ for $n = 8$. Superradiant states are shown in red, while subradiant states are in blue.

This analysis suggests a crude estimate of the instantaneous dissipation rate for a given n-qubit pure state. The collective angular momentum or Dicke-states form a complete basis, so an arbitrary n-qubit pure state can be expanded as

$$|\psi\rangle_S = \sum_{j,m,\alpha} a_{j,m,\alpha} |j,m,\alpha\rangle . \tag{48}$$

Define the *state-averaged collective enhancement factor*

$$\begin{aligned}\gamma_1 &= \sum_{j,m,\alpha} E(j,m) \left|a_{j,m,\alpha}\right|^2 = \sum_{j,m} E(j,m) \sum_{\alpha} \left|a_{j,m,\alpha}\right|^2 \\ &= \sum_{j,m} E(j,m) \sum_{\alpha} \left|\langle j,m,\alpha|\,\psi\rangle_S\right|^2 . \end{aligned} \tag{49}$$

A state with a large probability amplitude in the subradiant (superradiant) states will yield a small (large) value of γ_1. This suggests that states with large state-averaged collective enhancement factors interact strongly with the environment. Note that γ_1 is entirely determined by the probability weights for each (j,m) value, $\sum_\alpha |a_{j,m,\alpha}|^2$. These probability weights and the corresponding values of γ_1 are plotted for selected states $|\psi\rangle_S$ in Fig. 3.

For a given algorithm, in the absence of noise, the state evolves from an initial fiducial state $|\psi(0)\rangle$ to a final state $|\psi(T)\rangle$ according to the hamiltonian that generates the sequence of fundamental unitary gates. If we simulate the algorithm on a classical computer, the state-averaged collective enhancement factor $\gamma_1(t)$ can be calculated at each time in the interval $[0, T]$. This parameter is then proposed as an estimate of the instantaneous enhancement in the dissipation rate.

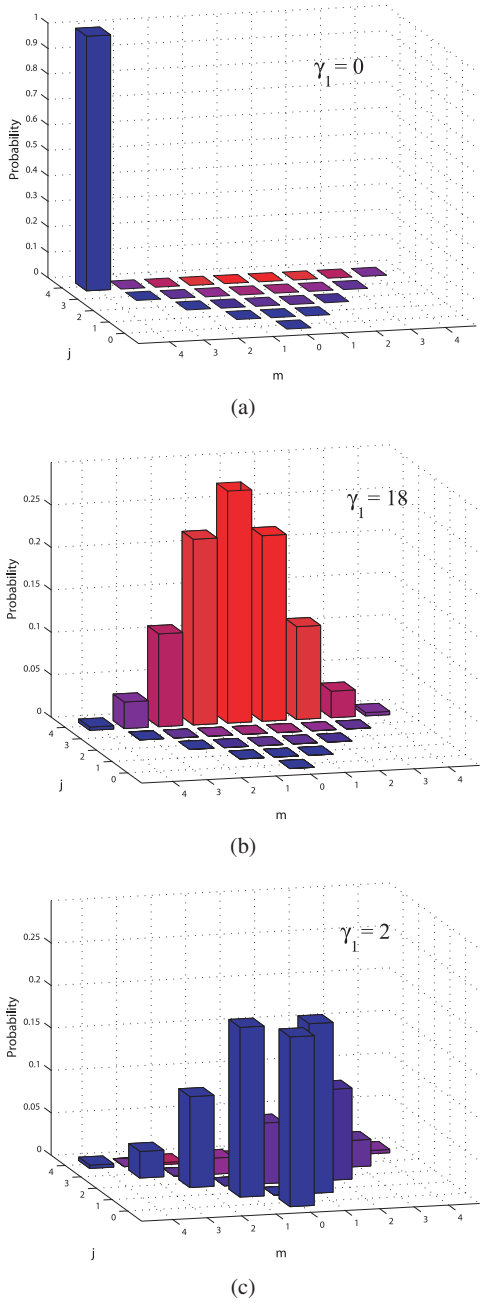

Fig. 3 Bar plots of the probability weights $\sum_\alpha |a_{j,m,\alpha}|^2$ for selected eight-qubit states, and the associated value of γ_1. Subradiant (DFS) states are dark blue, while superradiant states are bright red. (a) State $|j = 4, m = -4\rangle = |00000000\rangle$. (b) Equal superposition state $|\sigma\rangle \equiv (|0\rangle + |1\rangle)^{\otimes 8} / \sqrt{256}$. (c) Singlet-like superposition state $|\sigma'\rangle \equiv [(|0\rangle + |1\rangle) \otimes (|0\rangle - |1\rangle)]^{\otimes 4} / \sqrt{256}$.

We emphasize that γ_1 provides a *qualitative* estimate of the impact of collective decoherence, and does not necessarily correlate to a true physical dissipation rate[3].

3.4 Modifying the quantum search algorithm

Recall that to perform the quantum search algorithm, one first applies a Hadamard transformation $\hat{H}$ to all of n qubits to create the equally-weighted superposition state

$$|\sigma\rangle = \frac{1}{\sqrt{N}} \sum_{x=0}^{N-1} |\underline{x}\rangle . \tag{50}$$

Then, one repeatedly applies the operator $\hat{Q} = -\hat{H}\hat{U}_0\hat{H}\hat{U}_X$, where $\hat{U}_X$ and $\hat{U}_0$ are defined as

$$\hat{U}_X = \hat{I} - 2 \sum_{x\in X} |\underline{x}\rangle \langle \underline{x}| \tag{51a}$$

$$\hat{U}_0 = \hat{I} - 2 |\underline{0}\rangle \langle \underline{0}| . \tag{51b}$$

In the subspace spanned by $|\sigma\rangle$ and the state $|\bar{X}\rangle$, defined as

$$|\bar{X}\rangle = \frac{1}{\sqrt{r}} \sum_{x\in X} |\underline{x}\rangle , \tag{52}$$

$\hat{Q}$ can be interpreted as a rotation by a fixed angle θ, given in Eq. 9. After a given number of applications of $\hat{Q}$, the superposition state $|\sigma\rangle$ is rotated near $|\bar{X}\rangle$, and a projective measurement yields one of the solutions to the search problem with near certainty. The number of required rotations is $O(\sqrt{N/r})$.

Note in Fig. 3 (b) that the equal superposition state $|\sigma\rangle$ has a large state-averaged collective enhancement factor γ_1, as it exhibits a high probability weighting near the superradiant states[4]. Thus, in the initial part of the quantum search algorithm, as we start to rotate from $|\sigma\rangle$ towards $|\bar{X}\rangle$, we expect the dissipation rate to be high. It would be preferable if the algorithm could be carried out as a rotation in a different two-dimensional subspace, spanned by a subradiant state and $|\bar{X}\rangle$.

For example, consider replacing $|\sigma\rangle$ by the superposition state

$$\begin{aligned} |\sigma'\rangle &= \left(\frac{|0\rangle + |1\rangle}{\sqrt{2}}\right) \otimes \left(\frac{|0\rangle - |1\rangle}{\sqrt{2}}\right) \otimes \left(\frac{|0\rangle + |1\rangle}{\sqrt{2}}\right) \\ &\quad \otimes \left(\frac{|0\rangle - |1\rangle}{\sqrt{2}}\right) \otimes \cdots \\ &= \frac{1}{\sqrt{N}} \sum_{x=0}^{N-1} m(x) |\underline{x}\rangle , \end{aligned} \tag{53}$$

in which $m(x)$ keeps track of the minus signs inherent in expanding out the first line, and thus takes value ± 1. The state-averaged collective enhancement factor of $|\sigma'\rangle$ is given in Fig. 3 (c) for $n = 8$. The parameter γ_1 is substantially improved compared to $|\sigma\rangle$, due to the significant probability amplitude in subradiant states[5].

The modification required to change the invariant two-dimensional subspace is simple. Replace the Hadamard transformations in $\hat{Q}$ by the operator $\hat{V}_{mod}$, whose matrix representation in the computational basis is defined as

$$\begin{aligned} V_{mod} &= \frac{1}{\sqrt{2}} \begin{bmatrix} 1 & 1 \\ 1 & -1 \end{bmatrix} \otimes \frac{1}{\sqrt{2}} \begin{bmatrix} -1 & 1 \\ 1 & 1 \end{bmatrix} \\ &\quad \otimes \frac{1}{\sqrt{2}} \begin{bmatrix} 1 & 1 \\ 1 & -1 \end{bmatrix} \otimes \frac{1}{\sqrt{2}} \begin{bmatrix} -1 & 1 \\ 1 & 1 \end{bmatrix} \otimes \cdots \end{aligned} \tag{54}$$

Like the n-qubit Hadamard operator, $\hat{V}$ is a sequence of simple single-qubit gates on all n qubits. They differ only in the diagonal elements of the operators on alternating qubits.

To show that the operator $\hat{Q}_{mod} \equiv \hat{V}_{mod}\hat{U}_0\hat{V}_{mod}\hat{U}_X$ yields a rotation in the desired subspace, we recall the discussion of the generalized search algorithm. [34], [35] By Eqs. 12 through 15, the invariant subspace is spanned by

$$\hat{V}_{mod} |\underline{0}\rangle = |\sigma'\rangle \tag{55}$$

and

$$\begin{aligned} \sqrt{\frac{N}{r}} \sum_{x\in X} |\underline{x}\rangle \langle \underline{x}| \hat{V}_{mod} |\underline{0}\rangle &= \sqrt{\frac{N}{r}} \sum_{x\in X} |\underline{x}\rangle \langle \underline{x}| \sigma'\rangle \\ &= \frac{1}{\sqrt{r}} \sum_{x\in X} m(x) |\underline{x}\rangle . \end{aligned} \tag{56}$$

The rotation angle, given by Eq. 15, is

$$\theta = \sin^{-1}\left[2\sqrt{\sum_{x\in X} \left|\langle \underline{x}| \hat{V}_{mod} |\underline{0}\rangle\right|^2 - \left(\sum_{x\in X} \left|\langle \underline{x}| \hat{V}_{mod} |\underline{0}\rangle\right|^2\right)^2}\right]$$

[3] The reason for this is threefold. First, we have neglected the system hamiltonian $\hat{H}_S$ in the above discussion of transition rates. The control hamiltonian can influence and even eliminate the impact of system-environment coupling. Second, the state-averaged collective enhancement factor ignores phase information, as it averages over probabilities as opposed to probability amplitudes. Third, γ_1 is computed from the ideal trajectory of the state ket through the Hilbert space (i.e., the state in the absence of system-environment interaction). However, the system-environment coupling entangles the qubits with the reservoir, and the qubit state is correctly described by a reduced density matrix, tracing over the environmental degrees of freedom.

[4] As $|\sigma\rangle$ is symmetric under qubit permutations, only the maximal $j = n/2$ components have non-zero probability amplitudes.

[5] The small value of γ_1 for $|\sigma'\rangle$ can be understood by noting that $(|0\rangle + |1\rangle) \otimes (|0\rangle - |1\rangle) = |00\rangle - |11\rangle + |10\rangle - |01\rangle$. The states $|00\rangle$ and $|10\rangle - |01\rangle$ are the subradiant triplet and singlet states.

$$= \sin^{-1}\left[\frac{2\sqrt{r(N-r)}}{N}\right], \tag{57}$$

where we have noted that $\left|\left\langle \underline{x}\right| \hat{V}_{mod} \left|\underline{0}\right\rangle\right|^2 = \left[h(x)/\sqrt{N}\right]^2 = 1/N$. The angle in Eq. 57 is identical to that of the original algorithm (cf. Eq. 9).

In summary, the "modified algorithm" commences by applying $\hat{V}_{mod}$ to the initial state $\left|\underline{0}\right\rangle$, leading to $|\sigma'\rangle$. Successive applications of $\hat{Q}_{mod}$ rotate $|\sigma'\rangle$ towards the $\frac{1}{\sqrt{r}}\sum_{x\in X} m(x)\left|\underline{x}\right\rangle$ state. After $O(\sqrt{N/r})$ rotations, projective measurement yields one of the solutions in X with near-unity probability.

As the probability amplitudes of $|\sigma'\rangle$ in the collective angular momentum basis are large near the subradiant states, we intuit that the error induced by dissipation in the modified algorithm would be less than in the original algorithm. In the next section, we present simulation data of γ_1 for various instances of the search algorithm to bolster this claim.

3.5 Simulation data for the collective enhancement factor

In this section, we present simulation data of the state-averaged collective enhancement factor $\gamma_1(t)$ for instances of the original and modified quantum search algorithms. The simulations described in this section decompose a given instance of the search algorithm into a sequence of elementary gates, and then evaluate γ_1 after each gate. We first show how this decomposition is carried out for the original and modified algorithms. We then argue why it is reasonable to discretize the continuous function γ_1 after each fundamental gate. Last, we show simulation data for selected instances of the search problem.

As the fundamental gate set, we consider controlled-NOT (CNOT) gates along with arbitrary single-qubit operations. This choice is arbitrary, but it facilitates the simple decomposition of the operators required in the search algorithm. Each of the unitary operators in $\hat{Q} = -\hat{H}\hat{U}_0\hat{H}\hat{U}_X$ or $\hat{Q}_{mod} = -\hat{V}_{mod}\hat{U}_0\hat{V}_{mod}\hat{U}_X$ must be compiled into fundamental gates. The Hadamard and $\hat{V}_{mod}$ gates are straightforward; for the n-qubit search problem, each can be performed as a sequence of n elementary single-qubit gates. Recall that $\hat{U}_0$, defined in Eq. 51b, applies a phase-shift of π to the $\left|\underline{0}\right\rangle$ state, and leaves other computational basis states unmodified. Given an ancillary qubit initialized in the $(|0\rangle - |1\rangle)/\sqrt{2}$ state, $\hat{U}_0$ can be decomposed as shown in Fig. 4. The circuit requires $2n$ single-qubit gates and one "n-controlled-NOT" gate. The latter applies a NOT gate to the target ancillary qubit if all n control qubits are in the logical $|1\rangle$ state. Barenco et al. [40] presented

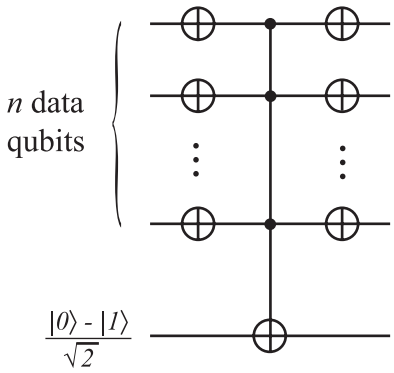

Fig. 4 A circuit to implement the $\hat{U}_0$ unitary operator on the n "data" qubits. The $\oplus$ symbols denote single-qubit NOT (bit-flip) gates that transform $|0\rangle \mapsto |1\rangle$ and $|1\rangle \mapsto |0\rangle$. The circuit applies a NOT gate to the ancillary qubit if all of the n other control qubits are in the $|0\rangle$ state. This maps $(|0\rangle - |1\rangle)/\sqrt{2}$ to $(|1\rangle - |0\rangle)/\sqrt{2} = -(|0\rangle - |1\rangle)/\sqrt{2}$, yielding the π-phase shift. Note that the ancillary bit remains unentangled.

three different methods to compile the n-controlled-NOT gate into elementary gates. In this work, we use the "Gray-code" decomposition, described in Ref. [40]. This method is best for small n when no additional work qubits are available.

For simplicity, we only consider instances of the quantum search algorithm where there is a single target state (i.e., $f(x) = 1$ for only a single input). The oracle $\hat{U}_X$ is then implemented in an identical fashion to $\hat{U}_0$; the only difference lies in the NOT gates that conjugate the n-controlled-NOT operator.

The simulation data were generated as follows. The n-qubit state vector consists of 2^n complex components, which are initialized to the $\left|\underline{0}\right\rangle$ state. The compiler breaks down the unitary operations required for the given instance of the search algorithm into fundamental gates. Each unitary elementary gate is applied to the state vector in sequence. After each gate, the state is projected on the Dicke-state basis and the state-averaged enhancement factor γ_1 is calculated. We implicitly assume that the evolution times for all single-qubit and CNOT gates are equal.

Note that this procedure computes γ_1 only at discrete times. However, one can argue that the variation of γ_1 over a gate time is small; solving for γ_1 after each fundamental gate is a reasonable approximation to the continuous function. To justify this assertion, note that a general n-qubit state can be expanded in the Dicke-state basis as Eq. 48. A unitary transformation $\hat{U}$ due to a single-qubit or CNOT gate maps $|\psi\rangle_S$ to

$$\hat{U}\,|\psi\rangle_S = \sum_{j',m',\alpha'} b_{j',m',\alpha'}\left|j',m',\alpha'\right\rangle \tag{58}$$

where

$$b_{j',m',\alpha'} = \sum_{j,m,\alpha} a_{j,m,\alpha} \langle j', m', \alpha' | \hat{U} | j, m, \alpha \rangle . \qquad (59)$$

As a consequence of the Wigner-Eckart theorem, [41]–[43] the matrix element in Eq. 59 is nonzero only for restricted values of $|j' - j|$ and $|m' - m|$. For a single qubit gate, $\langle j', m', \alpha' | \hat{U} | j, m, \alpha \rangle$ is zero unless both

$$\begin{aligned} |j' - j| &\leq 1, \\ |m' - m| &\leq 1. \end{aligned} \qquad (60)$$

To understand the consequence of this restriction, consider how a single-qubit gate can transform the graph of probability weights $\sum_\alpha |a_{j,m,\alpha}|^2$ for the $|\sigma\rangle$ state, shown in Fig. 3 (b). This state has a large value of γ_1 due to the significant superradiant components. After the application of a single-qubit gate, the probability weights are $\sum_{\alpha'} |b_{j',m',\alpha'}|^2$. By Eq. 60, $\hat{U}$ only couples the $a_{j,m,\alpha}$ probability amplitudes to $b_{j',m',\alpha'}$ coefficients that are represented by adjacent bars in Fig. 3. Thus, single-qubit gates only cause small "local" changes in the graph of probability weights, and lead to modest changes in γ_1.

Similarly, for CNOT gates, $\langle j', m', \alpha' | \hat{U} | j, m, \alpha \rangle$ is zero unless both

$$\begin{aligned} |j' - j| &\leq 2, \\ |m' - m| &\leq 1. \end{aligned} \qquad (61)$$

In Figs. 5 and 6, plots of γ_1 versus gate number are shown for an instance of the original and modified search algorithms, respectively. The data shown are for the seven-bit search algorithm with the target state $|\underline{0}\rangle = |0000000\rangle$; i.e., $\hat{U}_X = \hat{I} - 2|\underline{0}\rangle\langle\underline{0}|$. There are a total of $n = 8$ qubits, in addition to the seven "data" qubits, there is one ancillary qubit prepared in the $(|0\rangle - |1\rangle)/\sqrt{2}$ state to aid in constructing the $\hat{U}_0$ and $\hat{U}_X$ operators. For the seven-bit search algorithm, the rotation angle engendered by $\hat{Q}$ or $\hat{Q}_{mod}$ is 0.1770 (cf. Eq. 9). Eight invocations of $\hat{Q}$ (or $\hat{Q}_{mod}$) are required to rotate the initial $\hat{\sigma}$ state to the target state. Each $\hat{Q}$ (or $\hat{Q}_{mod}$) operation decomposes into 1316 fundamental gates; the dashed red vertical lines in the figures denote the beginning of each $\hat{Q}$ (or $\hat{Q}_{mod}$) operator.

The large-scale structure of Fig. 5 can be understood by a simple argument. The Hadamard gates at the very beginning of the algorithm place the seven data qubits in the equal superposition state,

$$|\sigma\rangle \equiv \frac{1}{\sqrt{2^7}} \sum_{x=0}^{2^7-1} |\underline{x}\rangle , \qquad (62)$$

which has a large superradiant component, and thus a large value of γ_1. Halfway through the first $\hat{Q} = -\hat{H}\hat{U}_0\hat{H}\hat{U}_X$ operator (near gate 660, when only $\hat{H}\hat{U}_X$

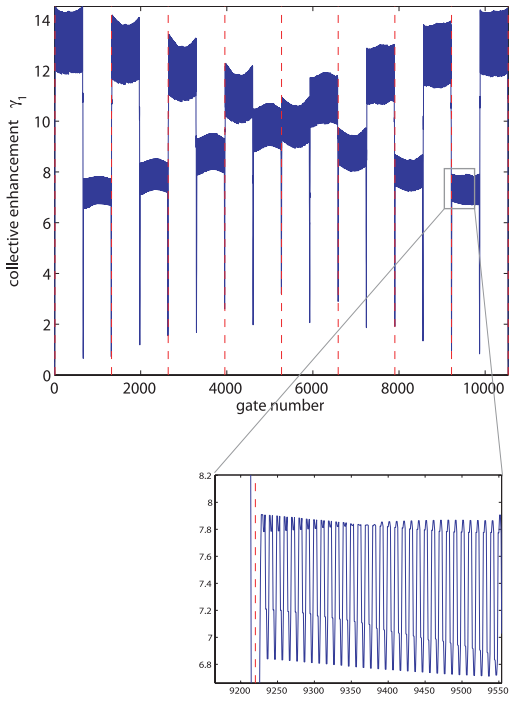

Fig. 5 Collective enhancement for the original seven-bit search algorithm with one ancillary qubit; the target state is $|0000000\rangle$ (i.e., $\hat{U}_X = \hat{I} - 2|0000000\rangle\langle 0000000|$). Red dashed lines indicate the beginning of each of the eight $\hat{Q}$ operators. As rapid variations in γ_1 cannot be resolved in the main plot, the expanded section is provided.

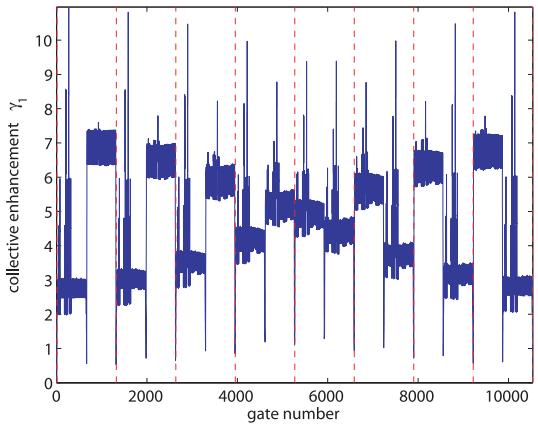

Fig. 6 Collective enhancement for the modified seven-bit search algorithm with one ancillary qubit; the target state is again $|0000000\rangle$.

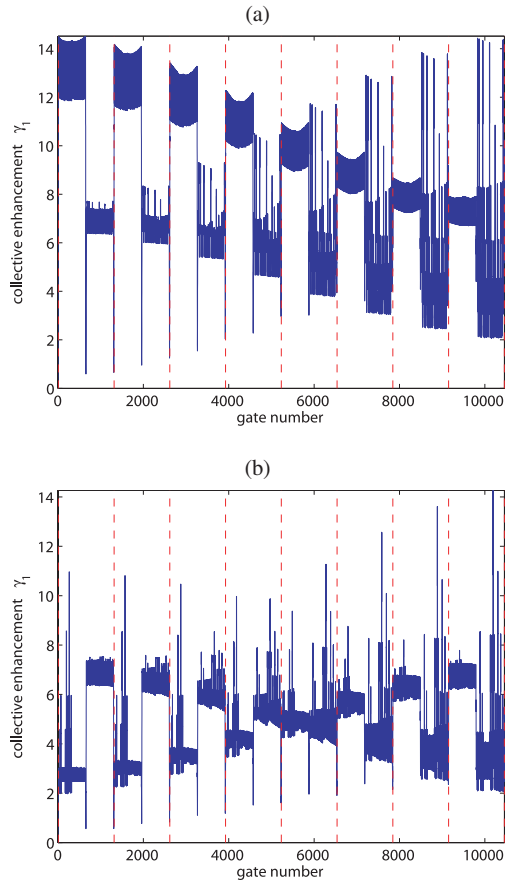

Fig. 7 Collective enhancement for the (a) original and (b) modified seven-bit search algorithm with one ancillary qubit; the target state is $|0001111\rangle$. The average collective enhancement factor $\overline{\gamma_1}$ is 8.00 for the original algorithm and 4.91 for the modified case.

has been applied), the value of γ_1 drops significantly. Note that

$$\begin{aligned}\hat{H}\hat{U}_X|\sigma\rangle &= \hat{H}\left(\hat{I} - 2\left|\underline{0}\right\rangle\left\langle\underline{0}\right|\right)|\sigma\rangle \\ &= \hat{H}\left(|\sigma\rangle - \frac{2}{\sqrt{2^7}}\left|\underline{0}\right\rangle\right) \\ &= \left|\underline{0}\right\rangle - \frac{2}{\sqrt{2^7}}|\sigma\rangle\,. \end{aligned} \tag{63}$$

The probability amplitude of the subradiant $\left|\underline{0}\right\rangle$ component is large, and it is not surprising that γ_1 decreases markedly. Now, consider γ_1 immediately after each invocation of $\hat{Q}$; i.e., to the right of each vertical red line. Each application of $\hat{Q}$ rotates the initial $|\sigma\rangle$ state towards the target $\left|\underline{0}\right\rangle$ state, and γ_1 steadily decreases.

Comparison of Figs. 5 (a) and 5 (b) show that the collective enhancement parameter γ_1 is significantly smaller for the modified algorithm compared to the initial algorithm. Let $\overline{\gamma_1}$ represent the average of γ_1 over all gates. For the original algorithm, $\overline{\gamma_1} = 10.28$, while $\overline{\gamma_1} = 4.74$ for the modified case.

As a further typical example, the collective enhancement factor is shown for the original and modified seven-bit search algorithm with target state $\left|\underline{31}\right\rangle = |0011111\rangle$ in Fig. 7. The modified algorithm improves the parameter $\overline{\gamma_1}$ from 8.00 to 4.91.

These two examples demonstrate the principle; further data is presented in Ref. [44]. In all simulations, the modified algorithm yielded a smaller gate-averaged collective enhancement factor.

4 Conclusion

We demonstrated that the quantum search algorithm can be modified to mitigate the impact of collective interaction with a boson reservoir on a qualitative parameter characterizing the dissipation rate. The modification was predicated on interpreting the quantum search algorithm as a rotation in a two-dimensional subspace, and selecting a subspace that diminishes the rate of the system-environment interaction via the gate decomposition.

Although the parameter used here to quantify dissipation is a simple first-order transition rate, simulations have been performed using a more rigorous quantum master equation approach. [44]

While the presented error-avoidance strategy is applicable to a specific algorithm and noise model, it illustrates the general importance of judicious decomposition of an algorithm into primitive gates. It is an open question whether it can be leveraged to improve the performance of other algorithms under more general noise models.

References

[1] P. W. Shor, "Scheme for reducing decoherence in quantum computer memory," *Phys. Rev. A*, vol.52, p.2493, 1995.

[2] A. M. Steane, "Error correcting codes in quantum theory," *Phys. Rev. Lett.*, vol.77, p.793, 1996.

[3] A. R. Calderbank and P. W. Shor, "Good quantum error-correcting codes exist," *Phys. Rev. A*, vol.54, p.1098, 1996.

[4] A. M. Steane, "Multiple particle interference and quantum error correction," *Proc. R. Soc. London A*, vol.452, p.2551, 1996.

[5] D. Gottesman, "Class of quantum error-correcting codes saturating the quantum Hamming bound," *Phys. Rev. A*, vol.54, p.1862, 1996.

[6] D. Gottesman, Ph.D. thesis, *Stabilizer Codes and Quantum Error Correction*, California Institute of Technology, 1997.

[7] E. Knill and R. Laflamme, "Power of One Bit of Quantum Information," *Phys. Rev. Lett.*, vol.81, p.5672, 1998.

[8] J. Preskill, "Reliable quantum computers," *Proc. R. Soc. London A*, vol.454, p.385, 1998.

[9] P. Zanardi, "Noiseless Quantum Codes," *Phys. Rev. Lett.*, vol.79, p.3306, 1997.

[10] P. Zanardi and M. Rasetti, "Error-avoiding codes," *Mod. Phys. Lett. B*, vol.11, p.1085, 1997.

[11] D. A. Lidar, I. L. Chuang, and K. B. Whaley, "Decoherence-Free Subspaces for Quantum Computation," *Phys. Rev. Lett.*, vol.81, p.2594, 1998.

[12] P. Zanardi, "Dissipation and decoherence in a quantum register," *Phys. Rev. A*, vol.57, p.3276, 1998.

[13] D. A. Lidar, D. Bacon, and K. B. Whaley, "Concatenating Decoherence-Free Subspaces with Quantum Error Correcting Codes," *Phys. Rev. Lett.*, vol.82, p.4556, 1999.

[14] D. A. Lidar and K. B. Whaley, *Decoherence-Free Subspaces and Subsystems*, in *Irreversible Quantum Dynamics*, Ed. F. Benatti and R. Floreanini, Springer-Verlag, Trieste, Italy, p.83, 2003.

[15] L. Viola and S. Lloyd, "Dynamical suppresion of decoherence in two-state quantum systems," *Phys. Rev. A*, vol.58, p.2733, 1998.

[16] L. Viola, E. Knill, and S. Lloyd, "Dynamical Decoupling of Open Quantum Systems," *Phys. Rev. Lett.*, vol.82, p.2417, 1999.

[17] L. Viola, S. Lloyd, and E. Knill, "Universal Control of Decoupled Quantum Systems," *Phys. Rev. Lett.*, vol.83, p.4888, 1999.

[18] L. Viola, E. Knill, and S. Lloyd, "Dynamical Generation of Noiseless Quantum Subsystems," *Phys. Rev. Lett.*, vol.85, p.3520, 2000.

[19] L. Viola and E. Knill, "Robust Dynamical Decoupling of Quantum Systems with Bounded Controls," *Phys. Rev. Lett.*, vol.90, p.037901, 2003.

[20] D. Aharonov, Ph.D. thesis, *Noisy Quantum Computation*, The Hebrew University, 1999.

[21] A. M. Turing, "On computable numbers, with an application to the Entscheidungsproblem," *Proc. London. Math. Soc.*, vol.2, p.230, 1936.

[22] C. H. Papadimitriou, *Computational Complexity*, Addison-Wesley, U.S.A., 1994.

[23] M. A. Nielsen and I. L. Chuang, *Quantum Computation and Quantum Information*, Cambridge University Press, U.K., 2000.

[24] D. Deutsch, "Quantum computational networks," *Proc. R. Soc. London A*, vol.425, p.73, 1989.

[25] C. H. Bennett, "Logical reversibility of computation," *IBM J. Res. Dev.*, vol.17, p.525, 1973.

[26] E. Fredkin and T. Toffoli, "Conservative Logic," *Int. J. Theor. Phys.*, vol.21, p.219, 1982.

[27] R. Cleve, A. Ekert, C. Macchiavello, and M. Mosca, "Quantum Algorithms Revisited," *Proc. R. Soc. London A*, vol.454, p.339, 1998.

[28] M. Mosca, Ph.D. thesis, *Quantum Computer Algorithms*, University of Oxford, 1999.

[29] P. W. Shor, "Polynomial-Time Algorithms for Prime Factorization and Discrete Logarithms on a Quantum Computer," in *Proc. of the 35th Annual Symposium on Foundations of Computer Science*, IEEE Computer Society Press, Santa Fe, NM, pp.124–134, 1994.

[30] P. W. Shor, "Polynomial-time algorithms for prime factorization and discrete logarithms on a quantum computer," *SIAM J. Comput.*, vol.26, p.1484, 1997.

[31] L. K. Grover, "A fast quantum mechanical algorithm for database search," in *Proc. of the Twenty-Eighth Annual Symposium on the Theory of Computing*, ACM Press, New York, pp.212–218, 1996.

[32] L. K. Grover, "Quantum Mechanics Helps in Searching for a Needle in a Haystack," *Phys. Rev. Lett.*, vol.79, p.325, 1997.

[33] M. Boyer, G. Brassard, P. Høyer, and A. Tapp, *Tight bounds on quantum searching* (1996), e-print quant-ph/9605034.

[34] G. Brassard and P. Høyer, "An Exact Quantum Polynomial-Time Algorithm for Simon's Problem," in *Proc. of the Fifth Israeli Symposium on the Theory of Computing and Systems*, IEEE Computer Society Press, p.12, 1997.

[35] L. K. Grover, "Quantum Computers Can Search Rapidly by Using Almost Any Transformation," *Phys. Rev. Lett.*, vol.80, p.4329, 1998.

[36] L. K. Grover, "A fast quantum mechanical algorithm for database search," in *Proc. of the Thirtieth Annual Symposium on the Theory of Computing*, ACM Press, New York, pp.53–62, 1998.

[37] D. F. Walls and G. J. Milburn, *Quantum Optics*, Springer-Verlag, Berlin, 1994.

[38] Y. Yamamoto and A. İmamoğlu, *Mesoscopic Quantum Optics*, Wiley, New York, 1999.

[39] R. H. Dicke, "Coherence in spontaneous radiation processes," *Phys. Rev.*, vol.93, p.99, 1954.

[40] A. Barenco, C. H. Bennett, R. Cleve, D. P. DiVincenzo, N. Margolus, P. Shor, T. Sleator, J. Smolin, and H. Weinfurter, "Elementary gates for quantum computation," *Phys. Rev. A*, vol.52, p.3457, 1995.

[41] C. Eckart, "The application of group theory to the quantum dynamics of monatomic systems," *Rev. Mod. Phys.*, vol.2, p.305, 1930.

[42] E. P. Wigner, *Gruppentheorie*, Vieweg, 1931.

[43] J. J. Sakurai, *Modern Quantum Mechanics*, Addison-Wesley, U.S.A., 1994.

[44] C. P. Master, Ph.D. thesis, *Quantum Computing Under Real-World Constraints*: *Efficiency of an Ensemble*

Quantum Algorithm and Fighting Decoherence by Gate Design, Stanford University, 2005.

Cyrus P. MASTER

Cyrus Master received the S.B. degree in Electrical Engineering and M.Eng. degree in Electrical Engineering and Computer Science from Massachusetts Institute of Technology in 1997 and 1998, respectively. He earned a Ph.D. in Electrical Engineering from Stanford University in 2005. He is currently a postdoctoral scholar jointly with the National Institute of Informatics and Stanford University. His current research focuses on the quantum many-body systems and quantum simulation.

Shoko UTSUNOMIYA

Received a B.S. degree in Electrical and Electric Engeneer from Tokyo Institute of Technology in 2003 and a M.S. in Information Science and Technology from the University of Tokyo in 2005. She is currently pursuing a Ph.D. degree at the University of Tokyo, where she does experimental and theoretical research in the field of Quantum Information under the supervision of Professor Yamamoto.

Yoshihisa YAMAMOTO

Received a B.S. from Tokyo Institute of Technology in 1973 and Ph.D. from the University of Tokyo in 1978, and has been working at Stanford University as a Professor of Applied Physics and Electrical Engineering since 1992 and at National Institute of Informatics as a Professor since 2003. He is also an NTT R&D Fellow, and a supervisor for the JST CREST program on quantum information. His current research areas include quantum optics, mesoscopic physics, solid-state NMR spectroscopy and quantum information.